

NON-LOCAL EFFECTS IN THE MEAN-FIELD DISC DYNAMO.

II. NUMERICAL AND ASYMPTOTIC SOLUTIONS

ASHLEY P. WILLIS*and ANVAR SHUKUROV

*School of Mathematics and Statistics, University of Newcastle,
Newcastle upon Tyne, NE1 7RU, UK*

ANDREW M. SOWARD

*Department of Mathematical Sciences, University of Exeter,
North Park Road, Exeter, EX4 4QE, UK*

DMITRY SOKOLOFF

Department of Physics, Moscow University, Moscow 119992, Russia

(Received 5 February 2008; in final form)

Abstract

The thin-disc global asymptotics are discussed for axisymmetric mean-field dynamos with vacuum boundary conditions allowing for non-local terms arising from a finite radial component of the mean magnetic field at the disc

*Now at School of Earth Sciences, University of Leeds.

surface. This leads to an integro-differential operator in the equation for the radial distribution of the mean magnetic field strength, $Q(r)$ in the disc plane at a distance r from its centre; an asymptotic form of its solution at large distances from the dynamo active region is obtained. Numerical solutions of the integro-differential equation confirm that the non-local effects act similarly to an enhanced magnetic diffusion. This leads to a wider radial distribution of the eigensolution and faster propagation of magnetic fronts, compared to solutions with the radial surface field neglected. Another result of non-local effects is a slowly decaying algebraic tail of the eigenfunctions outside the dynamo active region, $Q(r) \sim r^{-4}$, which is shown to persist in nonlinear solutions where α -quenching is included. The non-local nature of the solutions can affect the radial profile of the regular magnetic field in spiral galaxies and accretion discs at large distances from the centre.

KEY WORDS: Mean-field dynamos, thin-disc asymptotics, boundary conditions, galactic magnetic fields, accretion discs.

1 Introduction

Thin-disc asymptotics, applicable to spiral galaxies and accretion discs, have been a useful tool in the studies of the origin of large-scale magnetic fields in these objects. The small parameter naturally arising in a thin disc is its aspect ratio

$$\lambda \equiv h_0/R_0 \ll 1, \quad (1)$$

where h_0 and R_0 are the characteristic half-thickness and radius of the disc respectively. The height of the disc surface and the radius of its edge, understood as positions where suitable boundary conditions for the disc's magnetic field can be reasonably applied, are $h = O(h_0)$ and $R = O(R_0)$. In a domain that has no sharp boundaries (e.g., a plasma layer in hydrostatic equilibrium along the vertical direction and centrifugal equilibrium along radius), h_0 and R_0 can be identified with the scale height and the radial scale length, respectively.

We adopt cylindrical polar coordinates (r, ϕ, z) , in which z measures distance parallel to the rotation axis and assume that our system is axisymmetric, independent of the azimuthal angle ϕ . We assume that the mean motion is dominated by differential rotation and is approximated by the velocity $\mathbf{V} = (0, V, 0)$. We consider an axisymmetric magnetic field whose poloidal components can be expressed in terms of the azimuthal component A of the vector potential:

$$\mathbf{B} = \left(-\frac{\partial A}{\partial z}, B, \frac{1}{r} \frac{\partial}{\partial r}(rA) \right). \quad (2)$$

The magnetic field satisfies the mean-field dynamo equation

$$\frac{\partial \mathbf{B}}{\partial t} = \nabla \times (\mathbf{V} \times \mathbf{B} + \alpha \mathbf{B} - \beta \nabla \times \mathbf{B}) \quad (3)$$

(see Moffatt, 1978; Krause and Rädler, 1980), in which α and β are turbulent transport coefficients responsible for the α -effect and turbulent magnetic diffusion, respectively. We will consider the linear problem with V , α and β assumed given and independent of time t , for which solutions may be sought proportional to $\exp(\Gamma t)$, where the constant Γ is the growth rate.

The dynamo equation (3) has been solved with a non-local boundary condition, possible for an infinite slab, using the Bullard-Gellman (1954) formalism (Raedler and Wiedemann, 1990). Traditionally, however, the boundary conditions used in conjunction with (3) are the so-called vacuum boundary conditions. If there are no electric currents outside the disc, then $\nabla \times \mathbf{B} = \mathbf{0}$ there, and the magnetic field may be expressed as the gradient of a potential in the form $\mathbf{B} = -\nabla \Phi$. Thus the axial symmetry implies that the azimuthal magnetic field vanishes,

$$B = 0 \quad \text{outside the disc} \quad (4)$$

(see, e.g., Zeldovich *et al.*, 1983, p. 151), while the remaining meridional magnetic field is potential $\nabla^2 \Phi = 0$ since $\nabla \cdot \mathbf{B} = 0$. Our solution of the potential problem relies on two approximations. Firstly, we assume that the disc is so thin that its surface is essentially at $z = 0$. In this way we may obtain, using the Green's function,

a solution of the Neumann problem for $\Phi(r, z)$ in the upper half plane $z > 0$ in which the value of $B_z(r, 0_+) = -\partial\Phi/\partial z(r, 0_+)$ is specified. This Green's function solution may be used to calculate $B_r(r, 0_+) = -\partial\Phi/\partial r(r, 0_+)$. In terms of the vector potential A for the radial and axial magnetic field components $B_r = -\partial A/\partial z$ and $B_z = (1/r)\partial(rA)/\partial r$, the resulting expression for B_r in terms of B_z , both at $z = 0_+$, may be written in the form

$$\frac{\partial A}{\partial z}(r, 0_+) - \mathcal{L}\{A(r, 0_+)\} = 0, \quad (5)$$

where the operator

$$\mathcal{L}\{A(r, 0_+)\} = \frac{\partial}{\partial r} \left[\int_0^\infty G(r, r') \frac{\partial}{\partial r'} (r' A(r', 0_+)) dr' \right] \quad (6)$$

involves the Green's function

$$G(r, r') \equiv \frac{1}{2\pi} \int_{-\pi}^{\pi} \frac{d\theta}{\sqrt{r^2 - 2rr' \cos \theta + r'^2}}. \quad (7)$$

Secondly, we assume that the magnetic field is localised above the disc and is negligible beyond $r = R$. That means that the upper limit ∞ in the integral (6) is interchangeable with R . Then (5) is to be regarded as an equation that determines B_r as a nonlocal integral function of B_z on the disc surface $z = 0_+$ for vacuum boundary conditions. Indeed for the quadrupolar magnetic fields, which concern us in this paper, we also have $B_z(r, 0) = 0$ for $r > R$. For that case, no approximations are involved in interchanging ∞ with R .

In a previous paper, Priklonsky *et al.* (2000, hereafter referred to as Paper I) adopted the slightly different formulation

$$\mathcal{L}\{A(r, 0_+)\} = \frac{1}{r} \int_0^\infty W(r, r') \frac{\partial}{\partial r'} \left[\frac{1}{r'} \frac{\partial}{\partial r'} (r' A(r', 0_+)) \right] dr' \quad (8)$$

of the integral operator based on the solution of $(\nabla^2 - r^{-2})A = 0$ in the vacuum region outside the disc, where $W(r, r')$ will be given below, see (15). It is readily established by integration by parts that the operators (6) and (8) are equivalent provided that the two kernels $G(r, r')$ and $W(r, r')$ are related by

$$r \frac{\partial}{\partial r} [G(r, r')] = -\frac{1}{r'} \frac{\partial}{\partial r'} [W(r, r')]. \quad (9)$$

It is the latter formulation (8) that we employ to obtain our numerical results. The numerical implementation involves a regularisation procedure to allow for the singularity of the kernel, $W \approx -\pi^{-1}\sqrt{rr'} \ln|r-r'|$ at $r=r'$.

Inside thin discs, $|z| < h(r)$ on $0 \leq r < R$, where h may be a function of r , WKB type solutions of (3) can be constructed in the form

$$\begin{pmatrix} B \\ A \end{pmatrix} = \exp(\Gamma t) \left[Q(r) \begin{pmatrix} b(z; r) \\ a(z; r) \end{pmatrix} + \dots \right] \quad \text{with} \quad Q(r) = \widehat{Q}(r/\lambda^s) \quad (10)$$

(Soward, 1978, 1992a,b; Ruzmaikin *et al.*, 1985, 1988). The local z -structure on the short length scale h of the disc thickness, is determined by (b, a) normalised at our convenience; here z is measured in units of h so that the boundary is located at $z = \pm 1$. The corresponding time unit used to measure the inverse growth rate $1/\Gamma$ is h_0^2/β . The modulation on the long radial length scale R_0 , adopted as our unit of r , is quantified by the amplitude $Q(r)$. In our thin disc ($\lambda \ll 1$) the solution $\widehat{Q}(r/\lambda^s)$ is, in fact, usually modulated on a radial scale $\lambda^s R_0$ intermediate between R_0 and h_0 , where s is a constant satisfying $0 < s < 1$. The scale $\lambda^s R_0$ is large compared to the disc width, $h = O(\lambda R_0)$, but small compared to the disc radius, R , a quantity of order R_0 . The actual value taken by s depends on the nature of the boundary conditions. It is $s = 1/3$ for our non-local boundary condition (5) but may take other values if different boundary conditions are adopted; e.g., the value $s = 1/2$ found by Ruzmaikin *et al.* (1988) for a ‘local’ boundary condition as we explain below in relation to (14).

We note that generally the growth rate Γ of the dominant modes in a thin disc is real, when $\pm\alpha > 0$ for $\pm z > 0$. Raedler and Wiedemann (1990) considered non-local boundary conditions for an infinite slab, also finding that non-oscillatory modes are the most easily excited. The asymptotic expansion of the form (10) applies to modes of quadrupolar parity that dominate in galactic discs; dipolar modes, perhaps prevailing in accretion discs (e.g., Moss and Shukurov, 2003), have been discussed by Soward (1978, 1992a,b).

The lowest-order approximation in λ yields a boundary value problem for (b, a) that only involves derivatives in z and so is local in r . The local problem yields the local eigenfunction (b, a) together with its eigenvalue, namely the ‘local growth rate’ $\gamma(r)$ (see Paper I for details). Relative to local coordinates, in which the units of length for z and r are h and R_0 respectively ($z \rightarrow z/h$ and $r \rightarrow r/R_0$), the local eigenfunction determines a linear relation between $\partial a/\partial z(1; r)$ and $a(1; r)$ at the disc surface. We use dimensionless coordinates $z \rightarrow z/h$ and $r \rightarrow r/R_0$, keeping the notation z and r for them, unless stated otherwise. Used in conjunction with the boundary condition (5), the linear relation leads at next order to an amplitude equation governing $Q(r)$. Written in the form derived in Paper I, it is

$$[\Gamma - \gamma(r)] q(r) = \lambda \eta(r) \mathcal{L} \{q(r)\}, \quad (11)$$

where the factor λ reflects the fact that the radial unit of distance R_0 is a factor $1/\lambda$ larger than the axial unit h , the integral operator \mathcal{L} is defined by (8) with kernel $W(r, r')$ or (6) with kernel $G(r, r')$ and

$$q(r) = Q(r)a(1; r), \quad \eta(r) = \frac{a(1, r)a_*(1, r)}{\langle \mathbf{X}, \mathbf{X}_* \rangle}, \quad \mathbf{X} = \begin{bmatrix} b(z; r) \\ a(z; r) \end{bmatrix}. \quad (12)$$

Here \mathbf{X} is the eigenvector of the lowest-order boundary value problem, the asterisk denotes the eigenvector of its adjoint problem, while

$$\langle \mathbf{X}, \mathbf{X}_* \rangle = \int_0^1 \mathbf{X} \cdot \mathbf{X}_* dz.$$

The solution of (11) subject to the boundary conditions

$$q(0) = 0 \quad \text{and} \quad q \rightarrow 0 \quad \text{as} \quad r \uparrow \infty \quad (13)$$

provides yet another eigenvalue problem, for which the eigenvalue is the growth rate Γ and the eigenfunction is $q(r)$ which determines the radial r -modulation Q .

Soward (1978, 1992a,b) developed a systematic asymptotic theory for the marginally stable dynamo eigensolutions in a thin slab that includes the non-local coupling between its distant parts via the surrounding vacuum, as described by the integral

operator in (11) but in simplified local Cartesian rather than axisymmetric form. Though this theory was originally formulated in terms of Fourier transforms, real space formulation is given in (31) as obtained in Soward (2003). He pointed out, in particular, that the non-local coupling produces slowly decaying (algebraic) tails in the magnetic field radial distribution far away from the localization region of an eigenfunction. The corresponding theory with a full account for the cylindrical geometry and with allowance for growing (rather than steady) solutions was proposed in Paper I.

The integral term in (11) was neglected by Ruzmaikin *et al.* (1988), who were interested mainly in solutions within the dynamo active region, where the non-local external potential coupling may not be very important, so the integral term in (5) was neglected. Instead these authors included local internal coupling by diffusion, which leads to the radial dynamo equation

$$[\Gamma - \gamma(r)]Q = \lambda^2 \frac{\partial}{\partial r} \left[\frac{1}{r} \frac{\partial}{\partial r} (rQ(r)) \right] \quad (14)$$

similar to (11), but with the integral term replaced by the diffusion operator. The value of the exponent s in (10) is sensitive to this difference. If (14) is used, then $s = 1/2$ (Ruzmaikin *et al.*, 1985, 1988), whereas non-local asymptotics have $s = 1/3$ (Soward, 1978).

In this paper we discuss numerical solutions of the non-local radial equation (11), both in the kinematic regime and in a nonlinear regime with heuristically chosen nonlinearity. We compare solutions of the non-local equation (11) with those of the local equation (14), where the integral term is replaced by the diffusion operator, and confirm that the non-local coupling produces effects similar to enhanced radial diffusion. We also demonstrate that the algebraic tail of magnetic field outside the dynamo active region persists in nonlinear solutions.

Before continuing it must be emphasised that though it was convenient in (12) to measure the z -distance in units of h for the internal disc magnetic field, this is quite inappropriate in the vacuum region outside. So for the remainder of our paper

both z and r will be measured in units of R_0 , though we continue to write $a(1, r)$ for the value of a on the disc surface.

2 The Integral Kernel

In this section we develop various forms for the equivalent integral operators (6) and (8) employed in (11) which may be utilised effectively in our numerical methods as well as aid our understanding of the asymptotic results.

2.1 Properties of $G(r, r')$ and $W(r, r')$

We begin by noting that the kernels $G(r, r')$ and $W(r, r')$ in (6) and (8) have the integral representations

$$G(r, r') = \int_0^\infty J_0(kr) J_0(kr') dk, \quad W(r, r') = rr' \int_0^\infty J_1(kr) J_1(kr') dk \quad (15)$$

in terms of the Bessel functions $J_0(x)$ and $J_1(x)$ of the first kind. The equivalence of the former for $G(r, r')$ with (7) follows from Gradshteyn and Ryzhik's (2000), (3.674.1) and (6.512.1), and Abramowitz and Stegun's (1965), (17.3.9); henceforth referred to as G&R and A&S respectively. Further it is readily established using the elementary properties of the Bessel functions and their derivatives that the two kernels $G(r, r')$ and $W(r, r')$ are related by (9).

Significantly the kernels have the alternative representations

$$\left. \begin{aligned} G(r, r') &= \frac{2}{\pi r} K(m), \\ W(r, r') &= \frac{2r}{\pi} m \left[K(m) + 2(m-1) \frac{\partial K}{\partial m}(m) \right] \end{aligned} \right\} \quad \text{for } r' < r \quad (16)$$

in terms of the complete elliptic integral of the first kind

$$K(m) = \int_0^{\pi/2} \frac{d\theta}{\sqrt{1 - m \sin^2 \theta}} \quad \text{and} \quad m = \left(\frac{r'}{r} \right)^2 \quad (17)$$

(see G&R (6.512.1), A&S (15.2.7), (17.3.9)). Direct verification that $G(r, r')$ and $W(r, r')$ defined by (16) satisfy the relations (9) follows from the identity $4(d/dm)[m(1 -$

$m)dK/dm] = K$ (see G&R (8.124.1)). The forms for $r' > r$ are obtained using the symmetry relations

$$G(r, r') = G(r', r), \quad W(r, r') = W(r', r). \quad (18)$$

The asymptotic representations of the kernels are readily determined by documented properties of the complete elliptic integral. In particular use of the formula $2K(m) \approx \ln[16/(1-m)]$ valid when $1-m \ll 1$ (see A&S (17.3.26)) shows that the kernels $G(r, r')$ and $W(r, r')$ have the expansions

$$\left. \begin{aligned} G(r, r') &\approx \frac{1}{\pi r} \ln \left(\frac{8r}{r-r'} \right), \\ W(r, r') &\approx \frac{r}{\pi} \left[\ln \left(\frac{8r}{r-r'} \right) - 1 \right] \end{aligned} \right\} \quad \text{for } 0 < r - r' \ll r. \quad (19)$$

Likewise use of the formula $K(m) \approx (\pi/2)(1 + m/4)$ valid when $m \ll 1$ (see A&S (17.3.11)) shows that the kernel $G(r, r')$ has the expansion

$$G(r, r') \approx \frac{1}{r} + \frac{r'^2}{4r^3} \quad \text{for } r' \ll r. \quad (20)$$

Together these results determine the important asymptotic forms

$$\frac{\partial^2 G}{\partial r \partial r'}(r, r') \approx \begin{cases} -\frac{1}{\pi r(r-r')^2} & \text{for } 0 < r - r' \ll r, \\ -\frac{3r'}{2r^4} & \text{for } r' \ll r. \end{cases} \quad (21)$$

2.2 Asymptotic properties of localised solutions

In this section we discuss asymptotic forms of the solutions far from the dynamo active region. In particular, we clarify the nature of the slow, algebraic (rather than exponential) decay of the solution with cylindrical radius at large radii.

When $q(r)$ is localised about some point r_m on a length scale ϵ , where $\epsilon \ll r_m$, we integrate (6) by parts to obtain [noting that $A(r, 1) = q(r) \exp(\Gamma t)$]

$$\mathcal{L}\{q(r)\} = -\frac{\partial}{\partial r} \left[\int_0^\infty r' q(r') \frac{\partial}{\partial r'} [G(r, r')] dr' \right] \quad (22)$$

$$\approx -\mathcal{Q}r_m \frac{\partial G}{\partial r \partial r_m}(r, r_m) \quad \text{for } |r - r_m| \gg \epsilon, \quad (23)$$

where the slashed integral sign indicates principal part [needed here because $\partial G / \partial r' \sim (r - r')^{-1}$] and

$$\mathcal{Q} \equiv \int_0^\infty q(r) dr. \quad (24)$$

This result may be used in conjunction with (11) to obtain the far field behaviours

$$q(r) \approx -\frac{\lambda \eta(r) \mathcal{Q}}{\Gamma - \gamma(r)} r_m \frac{\partial^2 G}{\partial r \partial r_m}(r, r_m) \quad \text{for } |r - r_m| \gg \epsilon \quad (25)$$

of the modulation amplitude and the radial magnetic field

$$B_r(r, 1) \equiv -\frac{1}{\lambda} \frac{\partial A}{\partial z}(r, 1) \approx \exp(\Gamma t) \mathcal{Q} r_m \frac{\partial^2 G}{\partial r \partial r_m}(r, r_m) \quad \text{for } |r - r_m| \gg \epsilon \quad (26)$$

on the disc surface, as defined by (5). Furthermore from (21) we may employ the limiting forms

$$r_m \frac{\partial^2 G}{\partial r \partial r_m}(r, r_m) \approx \begin{cases} \frac{1}{\pi(r - r_m)^2} & \text{for } r_m \gg |r - r_m| \gg \epsilon, \\ \frac{3r_m^2}{2r^4} & \text{for } r \gg r_m. \end{cases} \quad (27)$$

The implication of the r -dependencies in (26) and (27) is that the response of the magnetic field in vacuum outside the disc corresponds to a line dipole source when $r_m \gg |r - r_m| \gg \epsilon$ but corresponds to a quadrupole source when $r \gg r_m$.

To illustrate the idea we consider the ‘local growth rate’

$$\gamma(r) = \gamma_m - \frac{1}{2} |\gamma_m''| (r_m - r)^2 \quad \text{on } 0 \leq r < \infty, \quad (28)$$

so that the influence of $\gamma(r)$ is dominated by its behaviour near r_m , where γ_m and γ_m'' are constants. Then the amplitude $q(r)$ governed by (11) satisfies

$$[(\Gamma - \gamma_m) + \frac{1}{2} |\gamma_m''| (r_m - r)^2] q(r) = \lambda \eta_m \mathcal{L}\{q(r)\}, \quad (29)$$

where $\eta_m \equiv \eta(r_m)$. Upon setting

$$r = r_m + \epsilon \varpi, \quad \Gamma = \gamma_m + \frac{1}{2} \epsilon^2 |\gamma_m''| \delta \quad \text{with } \epsilon = (2\lambda \eta_m / |\gamma_m''|)^{1/3}, \quad (30)$$

the integral equation (29) may be approximated for $\varpi = O(1)$ with the help of (19) and (22) to yield

$$(\delta + \varpi^2) \hat{q}(\varpi) \approx \frac{1}{\pi} \int_{-\infty}^{\infty} \frac{1}{\varpi' - \varpi} \frac{d\hat{q}}{d\varpi'}(\varpi') d\varpi', \quad (31)$$

where $\hat{q}(\varpi) = q(r)$. Here, since $\epsilon \ll 1$, the integration over $0 \leq r < \infty$ is equivalent asymptotically to $-\infty < \varpi < \infty$ on the basis that $\hat{q} \rightarrow 0$ as $|\varpi| \equiv |r - r_m|/\epsilon \rightarrow \infty$.

The lowest eigenvalue δ of the eigenvalue problem (31) given by Soward (2003) is $\delta \approx -1.0188$, namely the first zero of the derivative of Airy's function, $\text{Ai}'(\delta) = 0$. For that value we have the eigensolution

$$\hat{q}(\varpi) = \frac{\hat{\mathcal{Q}}}{\pi \text{Ai}(\delta)} \int_0^{\infty} \text{Ai}(k + \delta) \cos k\varpi dk, \quad (32)$$

where $\text{Ai}(\delta) \approx 0.53565$ and

$$\hat{\mathcal{Q}} = \int_{-\infty}^{\infty} \hat{q}(\varpi) d\varpi. \quad (33)$$

The large ϖ behaviour of \hat{q} is

$$\hat{q} \approx \frac{\hat{\mathcal{Q}}}{\varpi^4}. \quad (34)$$

This result is consistent with (25) and (27) provided that $r_m \gg |r - r_m| \gg \epsilon$.

3 Numerical results

In this section we discuss numerical solutions of the non-local radial equation (11) and assess the importance and implications of the non-local effects by comparing the solutions with those of its local ‘approximation’, (14). Our numerical solution of (11) employs the integral kernel $W(r, r')$ defined by (16). To that end $K(m)$ can be computed iteratively using the procedure of the arithmetic-geometric mean described in Sect. 17.6 of A&S, which displays phenomenal convergence. We also need to compute dK/dm ; for this, we use a modification of the above procedure described in Appendix A. Numerical solutions of the linear equation (11) and its nonlinear version, which we introduce in Section 3.3, involve a further regularization procedure described in Appendix B to contend with the singularity of the kernel.

The local dynamo problem at a fixed r , that yields the local growth rate $\gamma(r)$ and the local eigenfunction $(b(z; r), a(z; r))$, will not be solved here. Instead a suitable local growth rate, $\gamma(r)$, is prescribed and we take

$$a(1; r) = 1, \quad \eta(r) = \tilde{\eta}(r) = 1, \quad \text{so that} \quad q(r) = Q(r). \quad (35)$$

We adopt the boundary conditions

$$Q(0) = Q(R) = 0, \quad (36)$$

where R is the disc radius. Since our nonlocal integral equation (11) is derived for a disc of infinite radius, this may lead to an artificial boundary layer at $r = R$ if R is not large enough. Thus it is important that our magnetic field is localised and negligible for $r \geq R$. In the following subsections we consider examples of the cases in which $\gamma(r)$ is maximised on the symmetry axis $r_m = 0$ and also at a finite distance $r_m > 0$ from it.

3.1 Linear solutions for the case $r_m = 0$

The two leading eigenfunctions for the nonlocal (11) and local (14) eigenvalue problems are shown in Fig. 1 for the parabolic profile

$$\gamma(r) = \begin{cases} \gamma_m(1 - r^2/r_0^2), & r \leq r_0, \\ 0, & r > r_0 \end{cases} \quad (37)$$

with $\gamma_m = 10$, $r_m = 0$, $r_0 = 1$ and $R = 2$. The non-local eigenfunctions are broadened versions of the local solutions but their qualitative similarity is evident in Fig. 1. Such broadening of the eigenfunctions may be achieved from an anomalous, enhanced diffusion. For λ in the range applicable to spiral galaxies, namely $0.01 \lesssim \lambda \lesssim 0.1$, the eigenvalues Γ (growth rate) resulting from the non-local problem are smaller, while the eigenfunctions are generally wider – see Fig. 2. As might be expected, the non-local effects become weaker as λ decreases, i.e., as the disc becomes thinner.

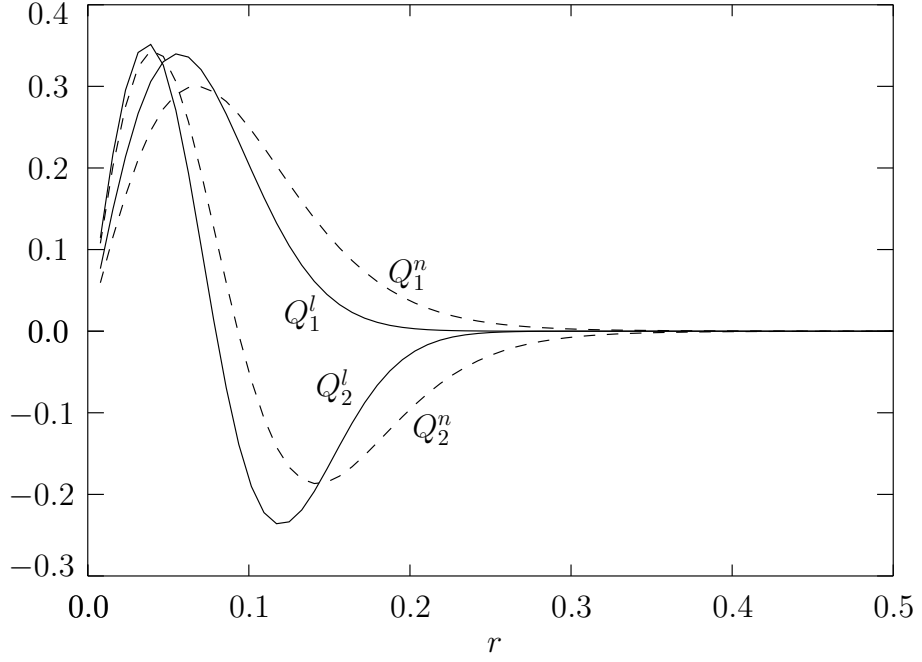


Figure 1: The first two eigenfunctions Q_1 and Q_2 of the local and non-local dynamo equations (14) and (11) respectively, for the case $\lambda = 0.01$ and $\gamma(r)$ of the form (37) with $\gamma_m = 10$, $r_0 = 1$ and $R = 2$. The local (non-local) eigenfunctions Q are shown with solid (dashed) curves and labelled with the superscript l (n).

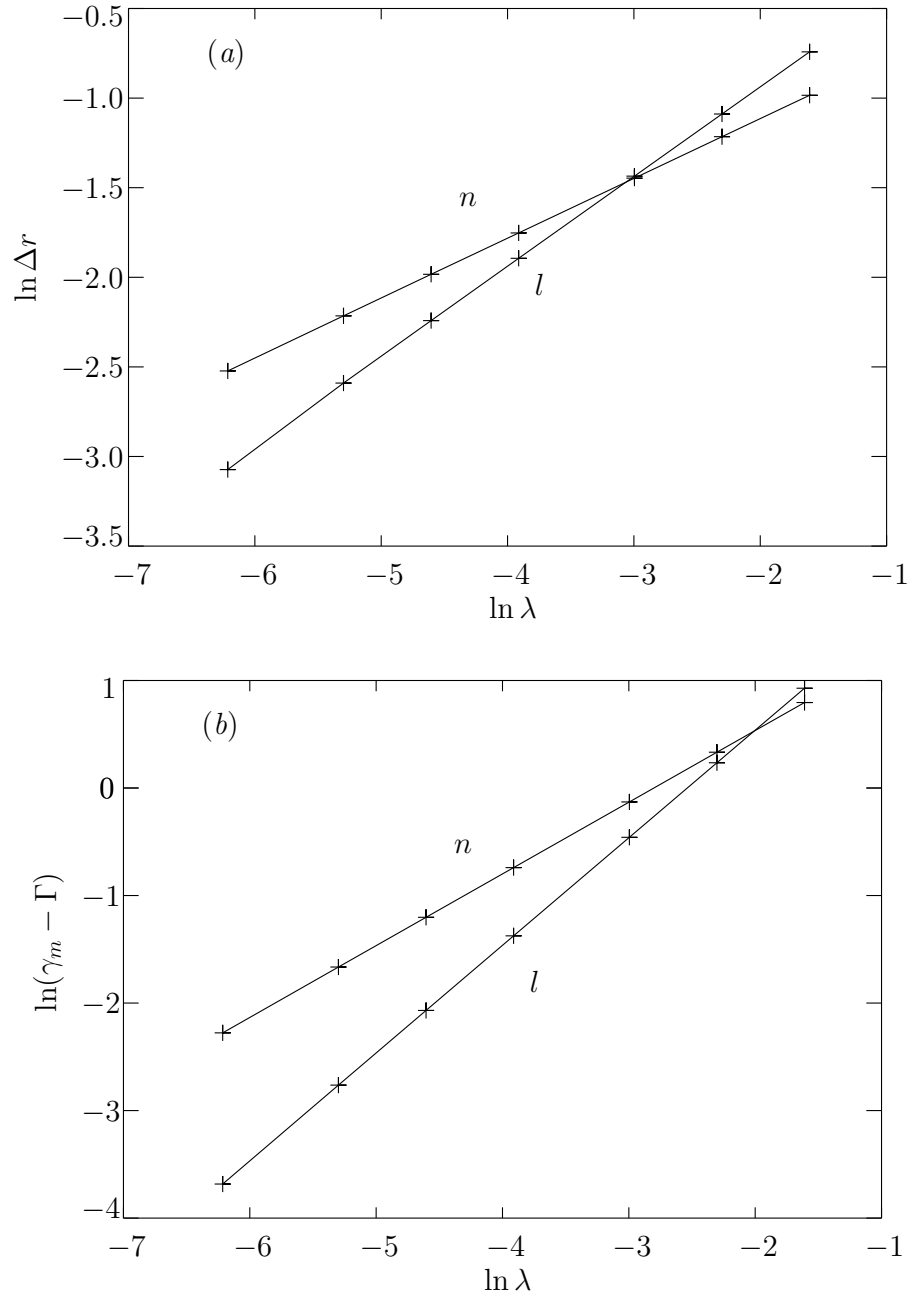


Figure 2: The dependencies of the leading eigensolutions on the dimensionless disc thickness λ showing the variations on a log-log scale: **(a)** the width of the eigenfunctions Δr (i.e., the distance between positions where $Q(r)$ decreases to e^{-1} of its maximum value) and **(b)** the decrement $\gamma_m - \Gamma$ of the eigenvalues. The local and non-local solutions are distinguished by labels l and n , respectively.

When $\gamma(r)$ is maximised off the disc axis, the eigenfunctions are localised in its vicinity on the length scale $\Delta r \propto \lambda^s$, while the corresponding eigenvalue decrement $\gamma_m - \Gamma$, which measures the growth rate Γ , scales as λ^{2s} . These two important qualitative measures of the non-local and local eigensolutions are distinguished by $s = 1/3$ and $s = 1/2$, respectively (see (30) and Paper I). Though these scalings are derived for our present case $r_m > 0$, they appear to hold also for the case $r_m = 0$ of Section 3.1 as Fig. 2 illustrates. Another important distinction of the non-local eigenfunctions is that they decay only algebraically at $r \rightarrow \infty$ (Soward, 1992a,b), in contrast to the exponential decay of the local eigenfunctions (e.g., Moss *et al.*, 1998).

As an illustrative example we consider the local growth rate

$$\gamma(r) = \begin{cases} \gamma_m r(2r_m - r)/r_m^2, & r \leq 2r_m, \\ \gamma_\infty, & r > 2r_m \end{cases} \quad (38)$$

similar to (28) with $\gamma_m'' = -2\gamma_m/r_m^2$ giving $\epsilon = (\lambda r_m^2)^{1/3}$. The leading eigenfunction for the parameter values $\lambda = 0.01$, $\gamma_m = 1$, $\gamma_\infty = 0$, $r_m = 0.25$ and $R = 4$ is shown in Fig. 3. Other values of γ_∞ are employed in Fig. 4 below.

We compare our eigenfunction with the asymptotic solution (32) valid close to r_m on the length scale $\epsilon = (\lambda r_m^2)^{1/3}$, shown with dashed curve in Fig. 3. For $\epsilon \ll |r - r_m| \ll r_m$ it determines the power law behaviour $Q \propto |r - r_m|^{-4}$ (see (34)) and this remains throughout the range $0 \leq r < 2r_m$ over which $\gamma(r)$ has a quadratic profile. This actually links to a line dipole source, for which the poloidal magnetic field decays as $|r - r_m|^{-2}$. For $r > 2r_m$, where $\gamma(r) = \gamma_\infty$ is a constant, we have instead (25), which takes the form

$$q(r) \approx -\frac{\lambda Q}{\gamma_m - \gamma_\infty} r_m \frac{\partial^2 G}{\partial r \partial r_m}(r, r_m), \quad (39)$$

where $r_m \partial^2 G / \partial r \partial r_m(r, r_m)$ has the asymptotic representation (27) giving

$$q(r) \approx \frac{3\lambda r_m^2 Q}{2(\gamma_m - \gamma_\infty)r^4} \quad (40)$$

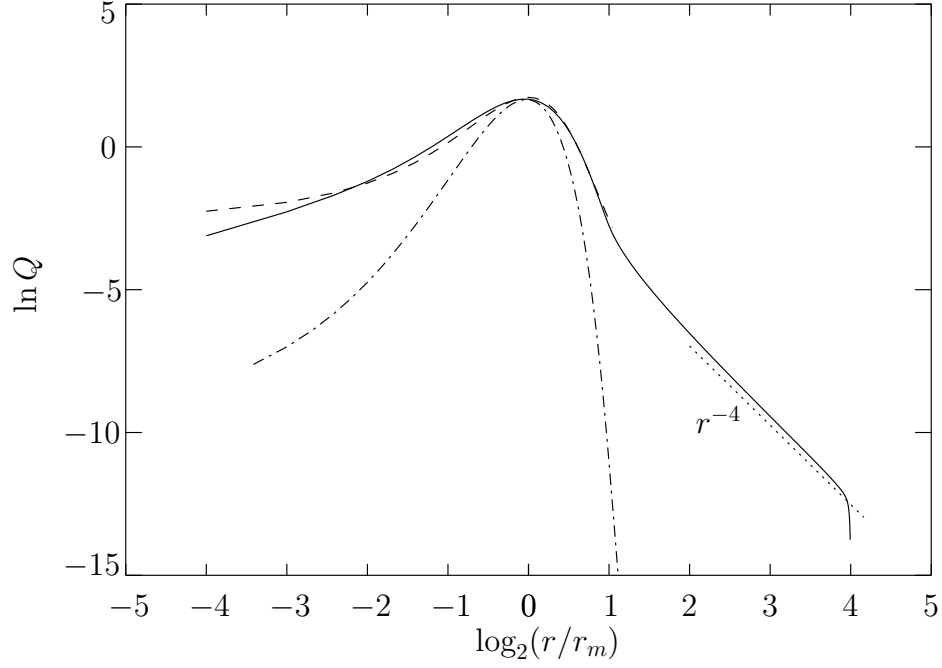


Figure 3: The leading eigenfunctions $Q(r)$ appropriate to $\gamma(r)$ defined by (38) with the parameter values $\lambda = 0.01$, $\gamma_m = 1$, $\gamma_\infty = 0$, $r_m = 0.25$ and $R = 4$ for the ‘local’ (14) (dash-dotted) and the non-local (11) (solid) problems; remember that $\gamma = \gamma_\infty$ on $1 < \log_2(r/r_m) < 4$. The local solution has an exponential tail for large $|r - r_m|$, whereas the non-local solution exhibits an algebraic tail. The dashed curve shows the WKB asymptotic solution (32) with the scaling (30). The dotted line shows the far field asymptote (34) or (40), valid for $r \gg 2r_m$.

similar to (27). This is the reason for the r^{-4} power law evident in Fig. 3 for $r > 2r_m$ and corresponds to the algebraic decay of its quadrupole source. This asymptotics improves as γ_∞ decreases, and the exponent -4 was generally found in the numerical results independent of the value of γ_∞ , at least for $\gamma_\infty \leq 0$.

The main points to note are that the asymptotic solution (32) generated by the Airy function approximates the numerical solution in the vicinity of r_m . The nature of Fig. 3 (namely, its relatively narrow relevant range in r) makes it impossible to easily identify the power law $|r - r_m|^{-4}$, given by (34), inside the source region $0 \leq r < 2r_m$. Whether or not it is there, the power law r^{-4} outside the source region $r > 2r_m$ has a different explanation for its similar power law exponent of -4 given by (40), specifically stemming from the quadrupole nature of the source. We also note that the horizontal and vertical components of magnetic field scale differently with r in the far field: $B \propto Q \propto r^{-4}$, $B_r = -\partial A / \partial z \propto r^{-4}$, and $B_z = r^{-1} \partial(rA) / \partial r \propto dQ / dr \propto r^{-5}$. Thus, the magnetic field becomes more horizontal with r at large distances from the dynamo active region.

3.3 Steady states

A simple heuristic form of nonlinearity in the radial dynamo equation (14), resulting from the standard form of α -quenching, $\alpha = \alpha_0 (1 + B^2 / B_0^2)^{-1}$, with α_0 the background unquenched value, was derived by Poezd *et al.* (1993) who suggest that $\gamma(r)$ is to be replaced by

$$\gamma^{(n)}(r, t) = \gamma(r) [1 - Q^2(r, t) / Q_0^2(r)], \quad (41)$$

where $Q_0(r)$ is essentially equal to B_0 , but with the possible z -dependence of B_0 averaged out. In this section, we compare the local and non-local steady states using this form with $Q_0(r) = 1$ in both (14) and (11), together with $\gamma(r)$ of the form (38) where γ_∞ was varied to explore properties of the solution at $r \gtrsim r_1$.

Taking the eigenfunctions of Sect. 3.2 as initial conditions, we solved the Cauchy problem for both the local and non-local dynamo equations using the Runge–Kutta

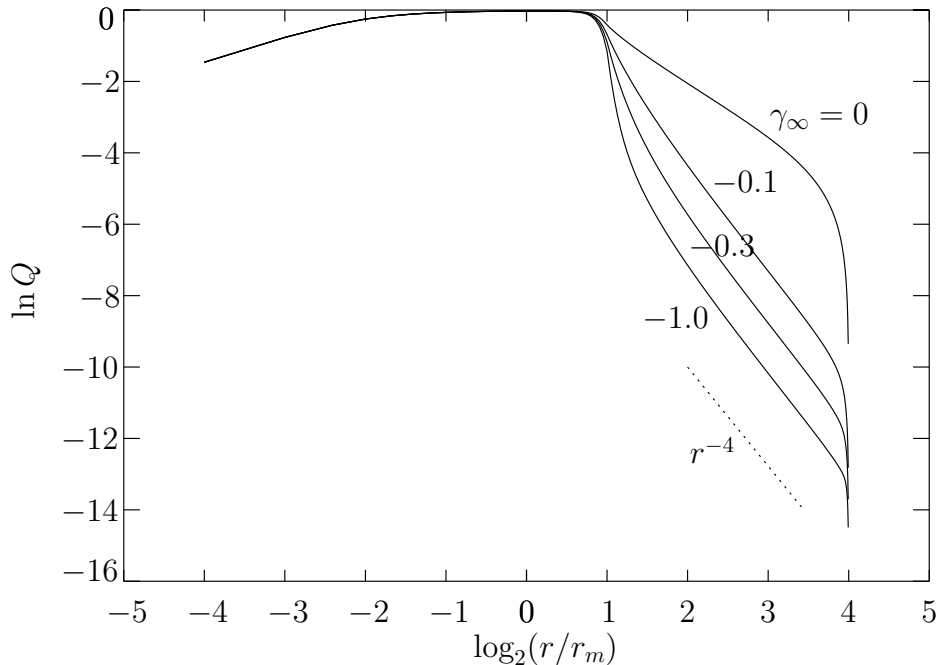


Figure 4: Steady-state nonlinear non-local solutions obtained for $\gamma(r)$ of the form (38) with $R = 4$, $r_m = 0.25$, $\lambda = 0.01$, and $\gamma_\infty = 0, -0.1, -0.3, -1.0$ (with the value of γ_∞ shown near the corresponding curve). The algebraic tail remains similar to that in the linear solutions, $Q \sim r^{-4}$, with the exponent independent of γ_∞ , although the magnitude of Q in the tail reduces as γ_∞ decreases.

method. This was performed also for the corresponding linear equation in order to verify the accuracy of the computations.

Figure 4 shows steady states for the non-linear regime. The non-linear solution clearly has a broader distribution in r than the associated eigenfunction in Fig. 3b. The algebraic tail $Q \sim r^{-4}$ characteristic of the non-local eigenmodes persists in the nonlinear solutions. Its functional form is independent of the local value of γ , as shown by our solutions with various values of γ_∞ . This is consistent with the fact that the algebraic tail results from the non-local magnetic connection with the dynamo-active region at smaller r . However, the magnitude of $Q(r)$ at large r is affected by the value of γ_∞ . This effect can be estimated from (25) with $\Gamma = 0$,

which yields $q(r) \propto Q/\gamma_\infty$. The values of q over the appropriate range of r in Fig. (4) agree with this to within 30% for $\gamma_\infty = -0.3$, and 20% for $\gamma_\infty = -1$.

3.4 Propagating Magnetic Fronts

If the local growth rate, $\gamma_0(r)$, is localized in a limited radial domain, growing magnetic field distribution of the local kinematic dynamo problem, (14), propagates at a finite velocity, V , into the dynamo-inactive region. This phenomenon was discussed by Moss *et al.* (1998, 2000), Petrov *et al.* (2001), Petrov (2002) and Fedotov *et al.* (2003). The eigenfunctions of (14) decay exponentially at large r , $Q(r) \propto \exp(\Gamma t - r/r_0)$, where $r_0 = (\beta/\Gamma)^{1/2}$ in dimensional variables. The position r_f where $Q = \text{const}$ changes with time as $r_f = r_0 \Gamma t = (\beta \Gamma)^{1/2} t$, i.e., the magnetic front propagates at a constant speed $V = (\Gamma \beta)^{1/2}$ (Moss *et al.*, 1998). The front propagation is strongly affected by the asymptotic behaviour of $Q(r)$ at $r \gg 1$: for the non-local solution, we have $Q \propto (r/r_0)^{-4} \exp(\Gamma t)$, so that $Q = \text{const}$ now yields $r_f = r_0 \exp \Gamma t / 4$, i.e., the magnetic front propagation is exponentially fast, with a speed increasing with time as $V \propto \exp \Gamma t / 4$. This is a direct consequence of the non-local coupling of the inner regions, where the dynamo is strong, with the outer regions where the front propagates: since magnetic fields propagates at infinite speed through vacuum, magnetic field far from the dynamo region responds instantaneously to the exponential growth of magnetic field in the inner parts of the disc.

These heuristic arguments are confirmed by numerical solutions illustrated in Fig. 5 where we show the position of the magnetic front defined here as a position $r = r_f$ where $Q(r_f) = 10^{-3}$. The eigenfunction of the nonlocal problem was used as the initial condition, normalised such that its maximum was 10^{-2} . The eigenfunction decreases with r relatively quickly for $r_m/2 < r < 2r_m$ (within the dynamo region) and then slower at $r > r_m$ (where $\gamma(r) = \gamma_\infty \leq 0$) — see Fig 3. Correspondingly, the front first propagates slowly through the region where the solution rapidly decreases

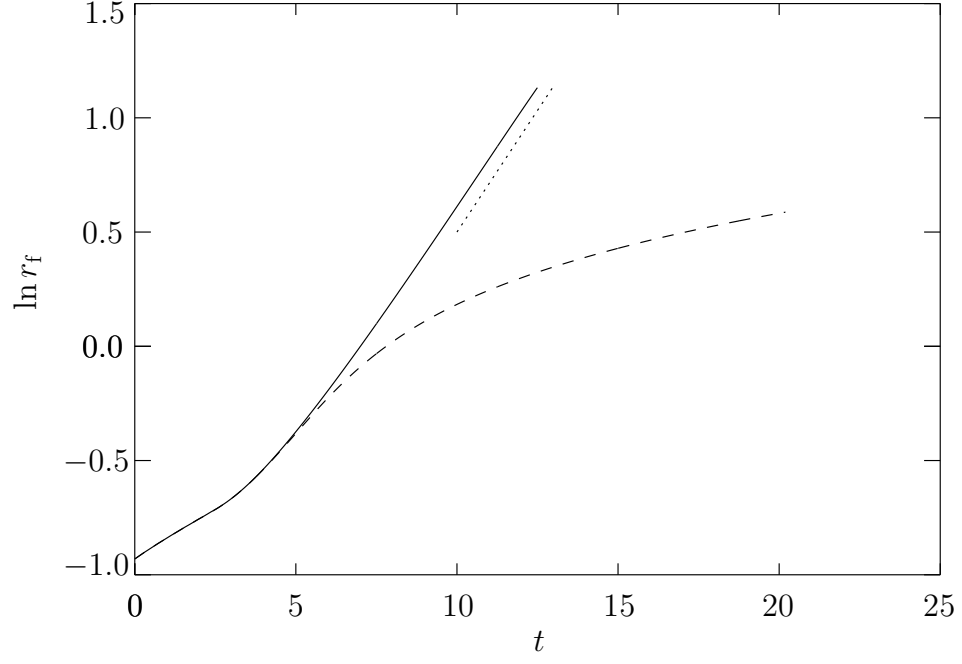


Figure 5: The position of a propagating magnetic front versus time for the linear (solid) and nonlinear (dashed) solutions of (11) with $\gamma(r)$ of the form (38) with the same parameters as in Fig. 3b and $\Gamma = 0.852$. The dotted line represents $\exp(\Gamma t/4)$.

away from its maximum, but the front speeds up as it reaches the region of the algebraic tail. Front propagation is inhibited by nonlinear effects as they suppress the exponential growth of the solution and then establish a steady state.

4 Conclusions and Discussion

Arguably the most important property of the non-local solutions discussed above is the slow, algebraic decay of both kinematic and steady-state mean magnetic fields at large distances, along radius, from the field maximum. This feature can be important for the understanding of large-scale magnetic fields observed at large distances from the centres of spiral galaxies where both low gas density and reduced intensity of interstellar turbulence would preclude any strong magnetic fields. However, Han *et al.* (1998) have found indications, albeit not very strong, that the large-scale magnetic field in the disc of the Andromeda nebula (M31) at distances as large as 25 kpc is almost as strong as at a radius of 10 kpc. Beck (2003) argues that magnetic field in the galaxy NGC 6946 (one of the better studied nearby spiral galaxies) decreases with galactocentric radius unexpectedly slowly, so it can become dynamically important in the outer Galaxy. If approximated by an exponential profile, the energy density of the total (regular plus random) magnetic field has the radial length scale of perhaps as large as 8 kpc. Meanwhile, the gas density decreases exponentially at a length scale of 2–3 kpc; if the turbulent velocity does not vary much with radius, this length scale applies to the turbulent energy density as well. Thus, the observations indicate that the large-scale magnetic field may decay with r slower than the turbulent energy density.

The algebraic tail produced by the non-local magnetic effects can be responsible for the slow decrease of the observed magnetic field with radius. It would be important to test this idea with numerical solutions for a disc dynamo embedded in a poorly conducting halo.

The assumption that the disc is surrounded by vacuum is essential for the nature

of the long-distance behaviour of the dynamo-generated magnetic field. Real galactic discs are surrounded by turbulent halos, and the vacuum boundary conditions are justified if the time scale of the (turbulent) magnetic field diffusion above the disc is significantly shorter than through the disc, i.e., if

$$\frac{\tau_h}{\tau_d} = \frac{\beta_d}{\beta_h} \frac{L^2}{R^2} \ll 1 ,$$

where β_h and β_d are the turbulent magnetic diffusivities in the halo and the disc, respectively, R is the radial length scale of the magnetic field in the disc, and L is the length of a magnetic line that leaves the disc through its surface and then returns to the disc with the radial distance R between its footpoints. As argued by Poezd *et al.* (1993), $\beta_h/\beta_d \simeq 10\text{--}30$, assuming that both the turbulent velocity and scale in the halo are 3–5 times larger than in the disc. With L/R of order unity, this yields $\tau_h/\tau_d \ll 1$; for $L/R \simeq 2$ we obtain $\tau_h/\tau_d \simeq 0.1\text{--}0.5$, a value arguably small enough to believe that the magnetic coupling through the halo is important.

Another condition for the algebraic tail to be established is that the magnetic propagation time through the halo is short enough in comparison with the galactic lifetime, $\tau_h \lesssim 10^{10}$ yr. Using for L the radial length scale of a kinematic non-local magnetic mode in the disc, $L \simeq \lambda^{-2/3}h$, i.e., assuming that the length of magnetic lines joining two positions in the disc through the halo does not differ strongly from the radial separation of the positions), where $h \simeq 500$ pc is the scale height of the galactic ionized disc and $\lambda = 0.05\text{--}0.1$ is its aspect ratio, we obtain $\tau_h \simeq (5\text{--}40) \times 10^8$ yr, with $\beta_h = (10\text{--}30)\beta_d$ and $\beta_d \simeq 10^{26} \text{ cm}^2 \text{ s}^{-1}$. Considering the uncertainty of the halo parameters, this estimate seems to indicate that the algebraic tail can be established in spiral galaxies, especially in those with strong halo turbulence or small disc.

We are grateful to W. Dobler for useful discussions. This work was supported by the Royal Society, the NATO collaborative research grant CRG1530959, and the PPARC Grant PPA/G/S/2000/00528.

References

- Abramowitz, M. and Stegun, I. A. (Eds), *Handbook of Mathematical Functions*, Dover Publ., New York (1965)
- Beck, R., “The Role of Magnetic Fields in Spiral Galaxies,” in: *From Observations to Self-Consistent Modelling of the ISM in Galaxies* (Eds M. Aivilez & D. Breitschwerdt), Kluwer, Astrophys. & Space Sci. Ser., in press (astro-ph/0212288) (2003).
- Bullard, G. E. and Gellman, H. “Homogeneous dynamos and terrestrial magnetism,” *Phil. Trans. R. Soc. Lond. A*, **250**, 543-585 (1954).
- Fedotov, S., Ivanov, A. and Zubarev, A., “Non-local mean-field dynamo theory and magnetic fronts in galaxies,” *Geophys. Astrophys. Fluid Dynam.*, **97**, 135-148 (2003).
- Gradshteyn, I. S. and Ryzhik, I. M. *Table of Integrals, Series and Products*, Academic Press (2000)
- Han, J. L., Beck, R. and Berkhuijsen E. M., “New clues to the magnetic field structure of M31,” *Astron. Astrophys.*, **335**, 1117–1123 (1998).
- Krause, F. and Rädler, K.-H., *Mean-Field Magnetohydrodynamics and Dynamo Theory*, Pergamon, Oxford (1980).
- Moffatt, H. K., *Magnetic Field Generation in Electrically Conducting Fluids*, Cambridge Univ. Press (1978).

- Moss, D., Petrov, A. and Sokoloff, D., “The motion of magnetic fronts in spiral galaxies,” *Geophys. Astrophys. Fluid Dynam.* **92**, 129–149 (2000).
- Moss, D. and Shukurov, A., “Accretion disc dynamos opened up by external magnetic fields,” *Astron. Astrophys.*, **413**, 403–414 (2004).
- Moss, D., Shukurov, A. and Sokoloff, D., “Boundary effects and propagating magnetic fronts in disc dynamos,” *Geophys. Astrophys. Fluid Dynam.* **89**, 285–308 (1998).
- Petrov, A. P., “Travelling contrast structures in various hydromagnetic dynamo models,” *Matematicheskoe Modelirovanie* **14**, 95–104 (2002) (in Russian).
- Petrov, A. P., Sokoloff, D. D. and Moss, D., “Magnetic fronts and two-component asymptotics for galactic magnetic fields,” *Astron. Zh.* **78**, 579–584 (2001). English translation: *Astron. Rep.*, **45**, 497–501 (2001).
- Poezd, A., Shukurov, A. and Sokoloff, D., “Global magnetic patterns in the Milky Way and the Andromeda nebula,” *Mon. Not. Roy. Astron. Soc.* **264**, 285–297 (1993).
- Press, W. H., Flannery, B. P., Teukolsky, S. A. and Vetterling, W. T., *Numerical Recipes*, Sect. 18.3.2, Cambridge Univ. Press, Cambridge (1993).
- Priklonsky, V., Shukurov, A., Sokoloff, D. and Soward, A., “Non-local effects in the mean-field disc dynamo. I. An asymptotic expansion,” *Geophys. Astrophys. Fluid Dynam.* **93**, 97–114 (2000). (Paper I.)
- Rädler, K.-H. and Wiedemann, E. “Mean field models of galactic dynamos admitting axisymmetric and non-axisymmetric magnetic field structures,” in: *Galactic and intergalactic magnetic fields* (Eds R. Beck, P. P. Kronberg & R. Wiełebinski), Kluwer, 107–112 (1990).

- Ruzmaikin, A. A., Shukurov, A. M. and Sokoloff, D. D., *Magnetic Fields of Galaxies*, Kluwer, Dordrecht (1988).
- Ruzmaikin, A. A., Sokoloff, D. D. and Shukurov, A. M., “Magnetic field distribution in spiral galaxies,” *Astron. Astrophys.* **148**, 335–343 (1985).
- Soward, A.M., “A thin disc model of the Galactic dynamo,” *Astron. Nachr.* **299**, 25–33 (1978).
- Soward, A.M., “Thin aspect ratio $\alpha\Omega$ -dynamos in galactic discs and stellar shells,” in: *Advances in Nonlinear Dynamos* (Eds A. Ferriz-Mas & M. Núñez), Taylor & Francis, London, pp. 224–268 (2003).
- Soward, A.M., “Thin disc $\alpha\omega$ -dynamo models. I. Long length scale modes,” *Geophys. Astrophys. Fluid Dynam.* **64**, 163–199 (1992a).
- Soward, A.M., “Thin disc $\alpha\omega$ -dynamo models II. Short length scale modes,” *Geophys. Astrophys. Fluid Dynam.* **64**, 201–225 (1992b).
- Zeldovich, Ya. B., Ruzmaikin, A. A. and Sokoloff, D. D., *The Almighty Chance*, World Scientific Publ., Singapore (1990).

Appendix A. The evaluation of the elliptic integral (17) and its derivative

To evaluate the elliptic integral (17), where we have introduced κ via $m = \sin^2 \kappa$, and used an iterative method described by Abramowitz and Stegun (1965): for the starting values

$$a_0 = 1, \quad b_0 = \cos \kappa = \sqrt{1 - m}, \quad (\text{A1})$$

we calculate

$$a_{n+1} = \frac{1}{2}(a_n + b_n), \quad b_{n+1} = \sqrt{a_n b_n} \quad (\text{A2})$$

to obtain

$$K(m) = \frac{\pi}{2a_\infty} . \quad (\text{A3})$$

The derivative dK/dm is calculated using a generalization of this algorithm suggested by W. Dobler (unpublished). We perturb the system above, $m \rightarrow m + \delta m$, $a_n \rightarrow a_n - \kappa_n \delta m$, $b_n \rightarrow b_n - \zeta_n \delta m$, where $\delta m \ll 1$. The starting values κ_0 and ζ_0 are obtained from the Taylor expansions of (A1):

$$\kappa_0 = 0 , \quad \zeta_0 = \frac{1}{2\sqrt{1-m}} ,$$

and similarly from (A2):

$$\kappa_{n+1} = \frac{1}{2}(\kappa_n + \zeta_n) , \quad \zeta_{n+1} = \frac{a_n \zeta_n + \kappa_n b_n}{2b_{n+1}} .$$

Perturbing (A3) with respect to m , we obtain

$$\frac{dK}{dm} = \frac{\pi}{2a_\infty^2} \kappa_\infty .$$

Typically, one or two iterations are sufficient to calculate $K(m)$, dK/dm to the eighth decimal place.

Appendix B. The regularization of the singular integral kernel $W(r, r')$, (15)

Equation (11) is solved numerically for $0 \leq r \leq R$, with suitably large R . The integral kernel of this equation, $W(r, r')$ has a singularity along the line $r = r'$. Simple quadrature methods may display poor convergence if such singularities are ignored and do not apply at $r = r'$. These difficulties are resolved using the subtraction of the singularity (Press *et al.*, 1993) by performing the following transformation:

$$\begin{aligned} [\Gamma - \gamma(r)]q(r) &= \frac{\lambda\eta(r)}{r} \int_0^R W(r, r') \widehat{L}_{r'}(q(r')) dr' \\ &= \frac{\lambda\eta(r)}{r} \left\{ \int_0^R W(r, r') \left[\widehat{L}_{r'}(q(r')) - \widehat{L}_r(q(r)) \right] dr' + \widehat{L}_r(q(r))M(r) \right\} , \quad (\text{B1}) \end{aligned}$$

where

$$\widehat{L}_r(q(r)) \equiv \frac{\partial}{\partial r} \left[\frac{1}{r} \frac{\partial}{\partial r} (rq(r)) \right],$$

$$M(r) \equiv \int_0^R W(r, r') dr' = r \int_0^R r' \left[\int_0^\infty J_1(kr) J_1(kr') dk \right] dr'. \quad (\text{B2})$$

As a result, the singularity in the integral operator at $r = r'$ is regularized since $\widehat{L}_{r'}(q(r')) - \widehat{L}_r(q(r)) = 0$ at $r = r'$. The additional term $\lambda\eta(r)M(r)r^{-1}\widehat{L}_r(q(r))$ describes a modified radial diffusion with diffusivity $\lambda\eta(r)M(r)r^{-1}$.

For finite, non-vanishing values of r , $M(r)$ can be calculated as follows. Making the substitution $\sigma = kr$, we obtain

$$M(r) = \int_0^R r' \left[\int_0^\infty J_1(\sigma) J_1(\sigma r'/r) d\sigma \right] dr'$$

and with $x = r'/r$ we find

$$M(r) = r^2 \int_0^{R/r} x \left[\int_0^\infty J_1(\sigma) J_1(\sigma x) d\sigma \right] dx = r^2 \widetilde{M}(r),$$

where

$$\widetilde{M}(r) = \int_0^{R/r} W(1, x) dx$$

is a universal function of r that need only be calculated once. For a mesh point r_n , $n \leq N$, $r_N = R$, we have

$$\begin{aligned} \widetilde{M}_N &= \int_0^1 W(1, x) dx, \\ \widetilde{M}_{n-1} &= \widetilde{M}_n + \int_{R/r_n}^{R/r_{n-1}} W(1, x) dx, \quad n = N, \dots, 2, \end{aligned} \quad (\text{B3})$$

where $\widetilde{M}_n = \widetilde{M}(r_n)$. Using an (open) quadrature method, we find $\widetilde{M}_N \approx 0.31409623$, the remaining \widetilde{M}_n , $n < N$ depend on the descretisation. From the recurrence relation (B3), \widetilde{M}_n , and hence M_n , may be precomputed by a single integration over the range 1 to R/r_1 .

We now take centered differences on the regularized equation (B1). The point $j = i$ in the corresponding sum is omitted since there $[\widehat{L}_{r_j}(q(r_j)) - \widehat{L}_{r_i}(q(r_i))] = 0$. This leads to the eigensystem $\Gamma \mathbf{Q} = A \mathbf{Q}$ which we solve using the QR algorithm.